Available online at www.sciencedirect.com
SCIENCE DIRECT®
Control Engineering Practice 12 (2004) 1017–1027
CONTROL ENGINEERING PRACTICE
www.elsevier.com/locate/conengprac

Optimal and robust feedback controller estimation for a vibrating plate ☆

Rufus Fraanje[a,*,1], Michel Verhaegen[a], Niek Doelman[b], Arthur Berkhoff[b]

[a] *Systems and Control Engineering Division, Faculty of Applied Physics, University of Twente, P.O. Box 217, NL-7500 AE Enschede, The Netherlands*

[b] *TNO TPD, P.O. Box 155, NL-2600 AD Delft, The Netherlands*

Received 27 August 2002; accepted 22 September 2003

Abstract

This paper presents a method to estimate the H_2 optimal and a robust feedback controller by means of Subspace Model Identification using the internal model control (IMC) approach. Using IMC an equivalent feed forward control problem is obtained, which is solved by the Causal Wiener filter for the H_2 optimal controller. The robust variant, called the Cautious Wiener filter, optimizes the *average performance* w.r.t. probabilistic model errors. The identification of the Causal and Cautious Wiener filters are *control-relevant*. The method is illustrated by experiments on a 4-inputs 4-outputs vibrating plate with additional mass variation.

Keywords: Active control; Robust control; Wiener filter; State space; Subspace methods

1. Introduction

Practical active vibration control (AVC) systems, should yield high suppression of disturbing vibrations, while still being robust against system and environmental variations. For example, as considered in this paper, a feedback controller counteracting the disturbing vibrations in a plate should not yield significant lower performance or even instability of the closed loop, if the mass load on the plate varies.

LQG/H_2 control (see e.g. Anderson & Moore, 1989) minimizes the mean square error (MSE) of the residual disturbances, but the model is assumed to be perfect, which leads in general to very poor stability robustness. Gradient-type adaptive algorithms, such as Filtered-X LMS (FxLMS) and Filtered-U LMS (FuLMS) have better robustness properties, but may lead to slow convergence and suboptimal performance in broadband MIMO applications (see e.g. Elliott, 2001).

In robust control literature, much attention has been paid to minimizing the H_∞ norm, in which model errors are taken into account explicitly (see e.g. Zhou, Doyle, & Glover, 1996). Though, stability robustness can be increased significantly, too often the performance is poor when optimizing for the worst case condition. Better performance is obtained by mixed H_2/H_∞ control design, where the H_2 performance measure is optimized subject to H_∞ constraints to guarantee user determined stability/performance robustness margins (see e.g. Bernstein & Haddad, 1989). More recently, a *minimax* LQG method was proposed by Petersen, Ugrinovskii, and Savkin (2000), which minimizes the MSE for the worst case model error (contained in a stochastic model uncertainty description). For more on robust H_2 control, see, e.g. Paganini (1999) and the references therein.

However, in all these robust design methods, the *likelihood* of the model errors is not taken into account. Such a design philosophy may be useful in critical applications where stability and a certain minimal (often low) level of performance should be guaranteed under all, including extremely rare, circumstances, e.g. in

☆This research has been conducted in the framework of the Knowledge Center 'Sound and Vibration UT-TNO', programme 'Robust Active Control' a joint initiative of TNO, Delft, The Netherlands and the University of Twente, Enschede, The Netherlands.

*Corresponding author.
E-mail address: r.fraanje@dcsc.tudelft.nl (R. Fraanje).
[1] Rufus Fraanje is currently visiting Delft University of Technology, Delft Center of Systems and Control, Mekelweg 2, 2628 CD, Delft, The Netherlands.

0967-0661/$ - see front matter © 2003 Elsevier Ltd. All rights reserved.
doi:10.1016/j.conengprac.2003.09.007

flight-by-wire control in aircrafts or biomedical control applications. Most active control problems are not that critical to pay a significant price on performance, and optimal performance on the *average* of all kind of model errors is desired. An additional reason is that most model identification methods give estimates of the likelihood of model errors, rather than hard bounds (see the discussion by Goodwin, Gevers, & Ninnes, 1992; Ljung, 1999). In this line Sternad and Ahlén (1993) proposed a probabilistic robust filtering/feed forward control method, which minimizes the MSE averaged over the (estimated) stochastic distribution of the model errors. The resulting robust filter is called a *Cautious* Wiener (CW) filter.

In this paper, the CW design philosophy is applied to *feedback* control systems via the well-known Internal Model Control (IMC) approach. It is also shown, via a small-gain theorem, that stability robustness is increased. Furthermore, the CW design problem is reformulated in an identification problem, which is approximately solved by e.g. Subspace Model Identification (SMI, Verhaegen, 1994) to obtain a state-space realization of the controller. This is done, because in AVC very high orders (here from 40 to 80) for the plant and the controller are used due to the large number of dominant modes. In such cases, the polynomial approach of Sternad and Ahlén (1993) (and Örn, 1996 for MIMO case) may lead to inaccurate and badly conditioned control design equations, especially for MIMO systems (see e.g. Gevers & Li, 1993). A second important advantage, is that the controller design problem is reformulated as a *control-relevant identification problem*. This means that the controller is estimated by directly minimizing the control cost function. The certainty equivalence principle is not valid in case of model uncertainty, which will reduce performance. Contrary, control-relevant identification takes model uncertainty into account in the optimal controller approximation.

The paper is organized as follows. Section 2 introduces notation and formulates the control problem. Sections 3 and 4 describe the estimation of the nominal and robust controller, respectively. Section 5 presents the validation of the methods on a vibrating plate experimental setup under two operating conditions: with and without additional mass mounted on the plate.

2. Notation and problem formulation

The notation $\mathbf{P}(q^{-1})$ indicates a discrete time LTI transfer function matrix and q^{-1} is the unit shift back operator. Usually $\mathbf{P}(q^{-1})$ is abbreviated with $\mathbf{P}$. The conjugate transpose of $\mathbf{P}$ is indicated by $\mathbf{P}^*(q^{-1}) = \mathbf{P}^{\mathrm{T}}(q)$ with q on the unit-circle in the complex-plane, $|q| = 1$. For a state-space realization $(\mathbf{A_p}, \mathbf{B_p}, \mathbf{C_p}, \mathbf{D_p})$ of $\mathbf{P}$, the transfer function matrix is $\mathbf{P}(q^{-1}) = \mathbf{D_p} + q^{-1}\mathbf{C_p}(\mathbf{I_n} - q^{-1}\mathbf{A_p})^{-1}\mathbf{B_p}$ with n the order of $\mathbf{P}$. $R_p^{M\times N}$ is the set of all rational proper $M \times N$ transfer function matrices. $RH_\infty^{M\times N}$ is the set of all asymptotically stable rational proper $M \times N$ transfer function matrices. So $\mathbf{P} \in RH_\infty^{M\times N}$ implies that all eigenvalues of $\mathbf{A_p}$ are in the open unit disc. The causality and the anti-causality operators are denoted as $[.]_+$ and $[.]_-$, respectively, see e.g. Elliott (2001). Note, that for every transfer function matrix $\mathbf{P}$ it holds that $\mathbf{P} = [\mathbf{P}]_+ + [\mathbf{P}]_-$ with $[\mathbf{P}]_+$ causal and stable and $[\mathbf{P}]_-$ strictly anti-causal (without direct feed through), and anti-stable. For example, let $\mathbf{P} \in RH$ be written as a Laurent series

$$\mathbf{P} = \sum_{i=-\infty}^{\infty} \mathbf{P_i} q^{-i},$$

then

$$[\mathbf{P}]_- = \sum_{i=-\infty}^{-1} \mathbf{P_i} q^{-i} \quad \in RH/RH_\infty,$$

$$[\mathbf{P}]_+ = \sum_{i=0}^{\infty} \mathbf{P_i} q^{-i} \quad \in RH_\infty.$$

The trace operator, which sums up the diagonal elements of a matrix, is indicated by tr(.) and stochastic expection by $E[.]$. Also the shorthand notations $(.)^*$ and $(.)^{\mathrm{T}}$ are used in multiplication with the same, but complex conjugate transposed and transposed factor, respectively.

Consider the standard block scheme of the feedback active control problem depicted in Fig. 1. The signal $\mathbf{s}(n) \in \mathbb{R}^M$ is the signal generated by the disturbance source. Assume $E[\mathbf{s}(n)] = \mathbf{0}$ and $E[\mathbf{s}(n)\mathbf{s}^{\mathrm{T}}(m)] = \mathbf{I_M}\delta(m-n)$ with $\delta(0) := 1$ and $\delta(n) := 0$ for $n \neq 0$, hence $\mathbf{s}$ is a white-noise stochastic process. The primary path and the secondary path are denoted by $\mathbf{P} \in RH_\infty^{M\times M}$ and $\mathbf{S} \in RH_\infty^{M\times K}$, respectively. The primary disturbance signal, denoted by $\mathbf{d}(n) \in \mathbb{R}^M$, is the disturbance signal which should be counteracted by the secondary signal $\mathbf{y}(n) \in \mathbb{R}^M$. The remaining disturbance is represented by the residual signal $\mathbf{e}(n) \in \mathbb{R}^M$, which is measured. The

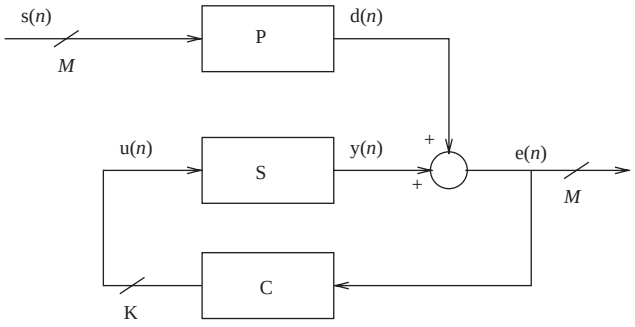

Fig. 1. Block scheme of the standard feedback disturbance rejection configuration.

control signal $\mathbf{u}(n) \in \mathbb{R}^K$ is calculated by the $K \times M$ controller $\mathbf{C}$ (not necessarily stable) using the measured residual signal. Hence, the plant is given by

$$\mathbf{e}(n) := \mathbf{P}\mathbf{s}(n) + \mathbf{S}\mathbf{u}(n) \tag{1}$$

and the control law by

$$\mathbf{u}(n) := \mathbf{C}\mathbf{e}(n). \tag{2}$$

The H_2 nominal controller design problem considered by e.g. Anderson and Moore (1989) is to minimize the cost function

$$J(\mathbf{C}) := \operatorname{tr} E[\mathbf{e}(n)\mathbf{e}^{\mathrm{T}}(n)] \tag{3}$$

subject to the constraint that $\mathbf{C}$ internally stabilizes the closed loop in Fig. 1.

The closed-loop in Fig. 1 can be stabilized by means of IMC, see Fig. 2. All internally stabilizing controllers are given by

$$\mathbf{C}(\mathbf{W},\mathbf{S}) = (\mathbf{I_K} + \mathbf{W}\mathbf{S})^{-1}\mathbf{W} \quad \text{with } \mathbf{W} \in RH_\infty^{M\times K}, \tag{4}$$

which is the Youla parameterization of the controller for stable $\mathbf{S}$. The stable filter $\mathbf{W}$ is called the Youla parameter, and we will determine this parameter for H_2 and for robust control. Note, that the control problem is reformulated as a *filtering problem*, which should be taken into account in case the model of $\mathbf{S}$ is not perfect, see Section 4.

The H_2 optimal controller, which minimizes Eq. (3) and stabilizes the closed-loop is given by Eq. (4) with $\mathbf{W}$ given by the Causal Wiener filter given by the following theorem.

Theorem 1 (Causal Wiener). *Let* $\mathbf{S} = \mathbf{S_i}\mathbf{S_o} \in RH_\infty^{M\times K}$ *with* $\mathbf{S_i} \in RH_\infty^{M\times L}$ *and* $\mathbf{S_o} \in RH_\infty^{L\times K}$ *with* $L \leqslant \min(K, M)$ *are the inner- and the outer-factor of* $\mathbf{S}$, *respectively, which are such that* $\mathbf{S} = \mathbf{S_i}\mathbf{S_o}$ *and* $\mathbf{S_i^*}\mathbf{S_i} = \mathbf{I_L}$ *and* $\mathbf{S_o^*}\mathbf{S_o} = \mathbf{S^*}\mathbf{S}$, $\mathbf{S_o}$ *has a stable right-inverse* $\mathbf{S_o^\dagger} \in RH_\infty^{K\times L}$. *Let* $\mathbf{P_o} \in RH_\infty^{M\times M}$ *be a minimum-phase spectral factor of* $\mathbf{P}$, *which is such that* $\mathbf{P_o}\mathbf{P_o^*} = \mathbf{P}\mathbf{P^*}$ *and* $\mathbf{P_o^{-1}} \in RH_\infty^{M\times M}$. *Then the closed-loop in Fig.* 1 *is internally stabilized and Eq.* (3) *is minimized by* $\mathbf{C}$ *given by Eq.* (4) *with* $\mathbf{W} = \mathbf{W_{H_2}}$ *given by*

$$\mathbf{W_{H_2}} = -\mathbf{S_o^\dagger}[\mathbf{S_i^*}\mathbf{P_o}]_+\mathbf{P_o^{-1}}, \tag{5}$$

which is called the Causal Wiener filter.

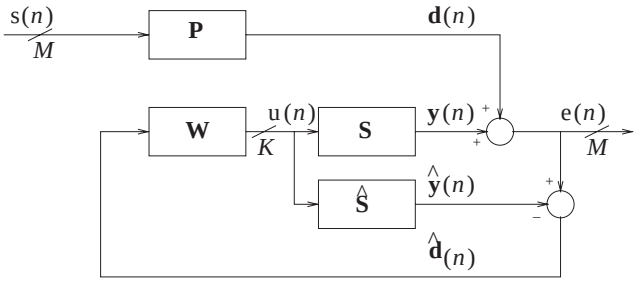

Fig. 2. Block scheme of the IMC controller, with internal model $\hat{\mathbf{S}}$.

Proof. For the proof of this theorem, see Vidyasagar (1985, Section 6.3). □

Note, if $\mathbf{S}$ has a stable right-inverse $\mathbf{S}^\dagger$, then $\mathbf{S_i} = \mathbf{I_M}$ and $\mathbf{W_{H_2}}$ reduces to $\mathbf{W_{H_2}} = -\mathbf{S}^\dagger$. However, in practice $\mathbf{S}$ does not have a stable right-inverse due to non-minimum phase zeros and delays from e.g. discretization, reconstruction and anti-aliasing filters.

3. Estimation of the nominal controller

This section describes three different methods to estimate the optimal filter given by (5), which yields an estimate of the optimal IMC controller given by (4). The first is the standard filter design fully based on the models of $\mathbf{S}$ and $\mathbf{P_o}$ and the principle of certainty equivalence.

The second method estimates the optimal filter by a prediction error model (PEM) identification method with output-error (OE) model structure, abbreviated as PEM-OE. The advantage of this approach is, that no spectral factor of the disturbance has to be estimated. Furthermore, if $\mathbf{S}$ is perfectly modeled, the cost function to be minimized in the *identification* problem equals the cost function to be minimized during *control*, and therefore called *control-relevant*.

Definition 2. An identification problem is said to be control-relevant if the cost function to be minimized for the identification equals the cost function to be minimized for control.

The third method makes use of Subspace Model Identification which has some computational advantages indicated below. Another identification problem has to be formulated, which needs an estimate of the spectral factor $\mathbf{P_o}$ but is still control-relevant.

3.1. Model based design

The secondary path $\mathbf{S}$ can be identified using a batch of measured data $\{\mathbf{u}(n), \mathbf{y}(n)\}_{n=1}^N$ measured by the error sensor(s) under the condition that $\mathbf{s}(n) = \mathbf{0}$ (this assumption can be weakened to the assumption that the process $\mathbf{s}(n)$ is independent of the process $\mathbf{u}(n)$). To obtain a state-space model for $\hat{\mathbf{S}}$ time-domain (Verhaegen, 1994) or frequency-domain (McKelvey, Fleming, & Moheimani, 2002) subspace identification can be used. The obtained estimate is denoted by $\hat{\mathbf{S}}$ and should be stable $\hat{\mathbf{S}} \in RH_\infty^{M\times K}$. The minimum phase spectral factor $\mathbf{P_o}$ can be estimated using a batch of measured data $\{\mathbf{d}(n)\}_{n=1}^N$ measured by the error sensor(s) under the condition that $\mathbf{u}(n) = \mathbf{0}$. A state-space realization of $\mathbf{P_o}$ can be estimated using stochastic subspace identification

methods, see e.g. Mari, Stoica, and McKelvey (2000). The obtained estimate is denoted by $\hat{\mathbf{P}}_\mathbf{o}$ and should be such that $\hat{\mathbf{P}}_\mathbf{o}, \hat{\mathbf{P}}_\mathbf{o}^{-1} \in RH_\infty^{M\times M}$, which can always be realized for non-singular spectra (i.e. $\mathbf{P_o P_o^*} > 0$, for $-\pi \leqslant \omega < \pi$). Note, that $\mathbf{S}$ and $\mathbf{P_o}$ can also be identified together by identification of a deterministic-stochastic model of $[\mathbf{S}\ \mathbf{P_o}]$. However, identification of $\mathbf{S}$ and $\mathbf{P_o}$ separately can be done with much higher accuracy because in the identification of $\mathbf{S}$ there is no disturbance from $\mathbf{s}(n)$ and vice verse. This conclusion was supported by experiments.

Using $\hat{\mathbf{S}}$ and $\hat{\mathbf{P}}_\mathbf{o}$ an estimate of the H_2 optimal filter can be made using Eq. (5)

$$\hat{\mathbf{W}}_{\mathbf{H}_2} = -\hat{\mathbf{S}}_\mathbf{o}^\dagger [\hat{\mathbf{S}}_\mathbf{i}^* \hat{\mathbf{P}}_\mathbf{o}]_+ \hat{\mathbf{P}}_\mathbf{o}^{-1}. \tag{6}$$

Due to model errors $\mathbf{C}(\hat{\mathbf{W}}_{\mathbf{H}_2}, \hat{\mathbf{S}})$ may not yield the optimal performance and may even destabilize the closed loop due to model errors in $\hat{\mathbf{S}}$. If we assume $\hat{\mathbf{S}}$ is perfectly modeled (robustness w.r.t. uncertainty in $\hat{\mathbf{S}}$ will be discussed in Section 4), then the closed loop is guaranteed to be stable because the controller is contained in the set of all stabilizing controllers given by (4). However, still optimal performance is not obtained due to model errors in $\hat{\mathbf{P}}_\mathbf{o}$.

3.2. Filter estimation by prediction error identification

The factor $[\mathbf{S}_\mathbf{i}^* \mathbf{P_o}]_+ \mathbf{P}_\mathbf{o}^{-1}$ in the Causal Wiener filter can be estimated by PEM-OE and restricting the model to be stable (Ljung, 1999). This is clear from noting, that

$$\begin{aligned}[\mathbf{S}_\mathbf{i}^* \mathbf{P_o}]_+ \mathbf{P}_\mathbf{o}^{-1} &= \arg \min_{\mathbf{X}\in RH_\infty^{L\times M}} \frac{1}{2\pi} \mathrm{tr} \int_{-\pi}^{\pi} (\mathbf{S}_\mathbf{i}^* \mathbf{P_o} - \mathbf{X P_o}) \\ &\quad \times (\mathbf{S}_\mathbf{i}^* \mathbf{P_o} - \mathbf{X P_o})^* \, \mathrm{d}\omega \\ &= \arg \min_{\mathbf{X}\in RH_\infty^{L\times M}} J_{id}(\mathbf{X})\end{aligned}$$

$$\text{with } J_{id} = \lim_{N\to\infty} \frac{1}{N} \sum_{n=1}^{N} (S_i^* d(n) - X d(n))(\cdot)^T \tag{7}$$

which can be inferred from Theorem 1 by setting $\mathbf{S_o} = \mathbf{I_L}$ (note that the power-spectral density of $\mathbf{d}(n)$ is given by $\mathbf{\Phi_d}(\omega) = \mathbf{P_o P_o^*}$). Hence, by restricting the model to be stable, the factor $[\mathbf{S}_\mathbf{i}^* \mathbf{P_o}]_+ \mathbf{P}_\mathbf{o}^{-1}$ is estimated by PEM-OE using the input/output data

$$\{\mathbf{d}(n), \mathbf{S}_\mathbf{i}^* \mathbf{d}(n)\}_{n=1}^N, \tag{8}$$

where the sequence $\{\mathbf{S}_\mathbf{i}^* \mathbf{d}(n)\}_{n=1}^N$ is generated by filtering *backwards* in time from $n = N$ to 1 because $\mathbf{S}_\mathbf{i}^*$ is strictly unstable.

The following lemma shows that the identification of the factor $\mathbf{X} = [\mathbf{S}_\mathbf{i}^* \mathbf{P_o}]_+ \mathbf{P}_\mathbf{o}^{-1}$ is control-relevant, because in the limit $N \to \infty$ (under reasonable conditions see Ljung, 1999) the cost function to be minimized in the identification equals (7) the cost function to be minimized during control (3).

Lemma 3. *Let* $\mathbf{S} \in RH_\infty^{M\times K}$ *be known, let* $\mathbf{X} \in RH_\infty^{L\times M}$ *and express* $\mathbf{C}$ *as given by Eq.* (4) *with* $\mathbf{W} \in RH_\infty^{K\times M}$ *equal to* $\mathbf{W}(\mathbf{X}) = -\mathbf{S}_\mathbf{o}^\dagger \mathbf{X}$.

Then minimizing Eq. (3) *over all* $\mathbf{X} \in RH_\infty^{L\times M}$ *is equivalent to minimizing Eq.* (7) *over all* $\mathbf{X} \in RH_\infty^{L\times M}$.

Proof. The proof is given in Appendix A.1. □

Let us discuss the advantage of estimating the factor $[\mathbf{S}_\mathbf{i}^* \mathbf{P_o}]_+ \mathbf{P}_\mathbf{o}^{-1}$ by PEM-OE over explicitly calculating $[\mathbf{S}_\mathbf{i}^* \hat{\mathbf{P}}_\mathbf{o}]_+ \hat{\mathbf{P}}_\mathbf{o}^{-1}$ as in Section 3.1. Often, it is difficult to estimate $\hat{\mathbf{P}}_\mathbf{o}$ accurately, especially its zeros. The model-errors in $\hat{\mathbf{P}}_\mathbf{o}$ will propagate in $[\mathbf{S}_\mathbf{i}^* \hat{\mathbf{P}}_\mathbf{o}]_+ \hat{\mathbf{P}}_\mathbf{o}^{-1}$ and leads to degradation of the performance. Also the estimate of $[\mathbf{S}_\mathbf{i}^* \mathbf{P_o}]_+ \mathbf{P}_\mathbf{o}^{-1}$ obtained by the identification approach of this section is contaminated with model errors and thus yields suboptimal performance. However, here $[\mathbf{S}_\mathbf{i}^* \mathbf{P_o}]_+ \mathbf{P}_\mathbf{o}^{-1}$ is estimated *directly* by minimizing the control cost function, and will usually lead to better performance compared with the *indirectly*, model-based approach.

The PEM-OE identification problem can be solved approximately by the `pem` tool implemented in the MATLAB System Identification Toolbox (Ljung, 2002). In the MIMO case, a state-space model of $[\mathbf{S}_\mathbf{i}^* \mathbf{P_o}]_+ \mathbf{P}_\mathbf{o}^{-1}$ is estimated by means of an iterative search, restricted to the domain of stable models (choose *Focus* = '*Simulation*') and initialized by the solution of a subspace identification method (see Verhaegen, 1994). To save computation time the calculation of the covariance of the parameter vector and the disturbance model were switched off. However, using this approach with the System Identification Toolbox the calculations are still very time consuming and no good accuracy could be obtained. For example, for a 4×4 system as considered in Section 5 with $N = 4000$ samples and of order 20, the calculation time was 25 min on a Pentium 4, 1500 MHz and the obtained MSE was only -7.3 dB (related to the power of the measured outputs). Note that no canonical forms of the state-space matrices should be constrained to prevent numerical problems (choose *SSParam* = '*Free*'). By increasing the order, the accuracy could not be improved. In comparison, the calculation time with the method of the next subsection was only 2 min and the model was significantly more accurate, the obtained MSE was -10 dB.

3.3. Filter estimation by subspace model identification

An attractive alternative for computationally complex multi variable system identification problems is to apply the subspace identification methods, as e.g. implemented in the SLICOT library (SLICOT, 2002). These methods

can be used only for causal/stable systems, but with the method of Verhaegen (1996) the tools can be adjusted easily to identify mixed causal/anti-causal systems.

However, if the input/output data (8) is used, the anti-causal system $\mathbf{S}_\mathbf{i}^*$ would be modeled instead of $[\mathbf{S}_\mathbf{i}^*\mathbf{P_o}]_+\mathbf{P_o}^{-1}$. In case $\mathbf{P_o}$ is known, a state-space realization of the factor $[\mathbf{S}_\mathbf{i}^*\mathbf{P_o}]_+$ can be estimated by the mixed causal/anti-causal subspace model identification method of Verhaegen (1996) using input/output data $\{\mathbf{P_o}^{-1}\mathbf{d}(n), \mathbf{S}_\mathbf{i}^*\mathbf{d}(n)\}_{n=1}^N$. In case only a model $\hat{\mathbf{P}}_\mathbf{o}$ of $\mathbf{P_o}$ is known $[\mathbf{S}_\mathbf{i}^*\mathbf{P_o}]_+$ is estimated using input/output data $\{\hat{\mathbf{P}}_\mathbf{o}^{-1}\mathbf{d}(n), \mathbf{S}_\mathbf{i}^*\mathbf{d}(n)\}_{n=1}^N$ and $\mathbf{W}$ is given by

$$\hat{\mathbf{W}}_{\mathbf{H_2,id}} = -\mathbf{S}_\mathbf{o}^\dagger\widehat{[\mathbf{S}_\mathbf{i}^*\mathbf{P_o}]}_+\hat{\mathbf{P}}_\mathbf{o}^{-1} \tag{9}$$

with $\widehat{[\mathbf{S}_\mathbf{i}^*\mathbf{P_o}]}_+$ denotes the estimate of $[\mathbf{S}_\mathbf{i}^*\mathbf{P_o}]_+$. Note, that even in case of model errors in $\hat{\mathbf{P}}_\mathbf{o}$, which result in non-white input sequence $\{\hat{\mathbf{P}}_\mathbf{o}^{-1}\mathbf{d}(n)\}_{n=1}^N$, the estimate $\widehat{[\mathbf{S}_\mathbf{i}^*\mathbf{P_o}]}_+$ is determined such that

$$\widehat{[\mathbf{S}_\mathbf{i}^*\mathbf{P_o}]}_+(\hat{\mathbf{P}}_\mathbf{o}^{-1}\mathbf{d}(n)) \approx \mathbf{S}_\mathbf{i}^*\mathbf{d}(n) \quad \text{for } n = 1, \ldots, N.$$

Again, it can be shown that the identification problem is control-relevant. The proof is similar to the proof of Lemma 3 and therefore not included here. This advantage over the *indirectly* model-based approach of Section 3.1 will be illustrated in the experiments of Section 5.

By explicitly evaluating the multiplications of the factors $\mathbf{S}_\mathbf{o}^\dagger$, $\widehat{[\mathbf{S}_\mathbf{i}^*\mathbf{P_o}]}_+$ and $\hat{\mathbf{P}}_\mathbf{o}^{-1}$ in Eq. (9), a very high order filter may be obtained (the sum of the orders of all factors). To circumvent this high order, an identification problem can be formulated to implicitly evaluate the multiplications in Eq. (9) by estimating a reduced order controller as explained by Fraanje, Verhaegen, and Doelman (2001).

4. Robust controller design

4.1. Derivation of the robust controller expression

In designing the nominal filter, it is assumed that the secondary path $\mathbf{S}$ was perfectly modeled. However, this assumption is not valid in practical Active Control systems. Therefore, this section shows how to estimate a robust filter $\mathbf{W_{CW}}$ (Cautious Wiener filter), where $\mathbf{W_{CW}}$ will replace $\mathbf{W}$ in Fig. 2, such that the controller $\mathbf{C}(\mathbf{W_{CW}}, \hat{\mathbf{S}})$ yields robust performance and robust stability w.r.t. secondary path model errors $\Delta\mathbf{S}$ given as $\Delta\mathbf{S} := \mathbf{S} - \hat{\mathbf{S}}$.

In the Cautious Wiener design philosophy of Sternad and Ahlén (1993) and Örn (1996) the uncertainty on the secondary path model $\Delta\mathbf{S}$ is modeled as a stochastic variable (see also Goodwin, Gevers, & Ninnes, 1992) independent of $\mathbf{s}(n)$, $\mathbf{P}$ and $\hat{\mathbf{S}}$ and such that

$$\bar{E}[\Delta\mathbf{S}(e^{-j\omega})] = \mathbf{0}, \quad -\pi \leqslant \omega < \pi, \tag{10}$$

$$\bar{E}[\Delta\mathbf{S}(e^{-j\omega})\Delta\mathbf{S}(e^{-j\omega})^*] = \mathbf{\Phi}_{\Delta\mathbf{S}}(e^{-j\omega}), \quad -\pi \leqslant \omega < \pi, \tag{11}$$

$\mathbf{\Phi}_{\Delta\mathbf{S}}(e^{-j\omega}) > 0$, $-\pi \leqslant \omega < \pi$ is given and $\bar{E}[.]$ the expectation operator over $\Delta\mathbf{S}$. The only difference with (Sternad and Ahlén, 1993; Goodwin et al., 1992) is that we will assume a *state-space* model estimate of a stable spectral factor of $\mathbf{\Phi}_{\Delta\mathbf{S}}$ is available rather than the covariance matrix of polynomial filter coefficients. During control design, it can be assumed that the disturbance signal $\mathbf{d}(n)$ can be measured (set $\mathbf{u}(n) = \mathbf{0}$), such that the following feed forward control problem is obtained. Let the plant equations be given by

$$\mathbf{e}(n) = \mathbf{P}\mathbf{s}(n) + (\hat{\mathbf{S}} + \Delta\mathbf{S})\mathbf{u}(n), \tag{12}$$

$$\mathbf{d}(n) = \mathbf{P}\mathbf{s}(n) \tag{13}$$

and the control-law by

$$\mathbf{u}(n) = \mathbf{W_{CW}}\mathbf{d}(n). \tag{14}$$

Then the robust filter problem is to design $\mathbf{W_{CW}} \in RH_\infty^{K\times M}$ such that the robust cost function

$$J_{\text{rob}} = \text{tr}\,\bar{E}\bar{E}[\mathbf{e}(n)\mathbf{e}^{\mathrm{T}}(n)] \tag{15}$$

is minimized. This problem is solved in the following theorem.

Theorem 4 (Cautious Wiener filter). *Let the plant equations be given by Eqs.* (12) *and* (13) *with* $\Delta\mathbf{S}$ *a stochastic variable satisfying Eqs.* (10) *and* (11). *Let the spectral factor* $\widetilde{\Delta\mathbf{S}} \in RH_\infty^{M\times M}$ *of* $\widetilde{\Delta\mathbf{S}}^*\widetilde{\Delta\mathbf{S}} = \mathbf{\Phi}_{\Delta\mathbf{S}}$ *be given, define the following augmented primary and secondary paths*

$$\mathbf{P_o^{aug}} := \begin{bmatrix} \mathbf{P_o} \\ \mathbf{0_{M\times M}} \end{bmatrix}, \quad \mathbf{S^{aug}} := \begin{bmatrix} \hat{\mathbf{S}} \\ \widetilde{\Delta\mathbf{S}} \end{bmatrix}$$

and let $\mathbf{S_i^{aug}}\mathbf{S_o^{aug}}$ *be an inner–outer factorization of* $\mathbf{S^{aug}}$. *Then the control-law Eq.* (14) *minimizes* Eq. (15) *if* $\mathbf{W_{CW}}$ *is given by*

$$\mathbf{W_{CW}} = -\mathbf{S_o^{aug\dagger}}[\mathbf{S_i^{aug*}}\mathbf{P_o^{aug}}]_+\mathbf{P_o}^{-1}, \tag{16}$$

which is called the Cautious Wiener filter.

Proof. For the proof see Appendix A.2. □

From the proof (Eq. (A.1)), it is directly inferred that by minimizing the robust cost function (15) the gain of the filter $\mathbf{W_{CW}}$ is decreased in the frequency region where the uncertainty in the secondary path is large (i.e. $\mathbf{\Phi}_{\Delta\mathbf{S}}$), hence the influence of the uncertainty on $\mathbf{e}(n)$ will be reduced. The robust controller is determined by a frequency-dependent regularized optimization problem.

Furthermore, Eq. (16) can be reduced to

$$\mathbf{W_{CW}} = -\mathbf{S_o^{aug\dagger}}[\mathbf{S_{i1}^{aug*}}\mathbf{P_o}]_+\mathbf{P_o}^{-1}$$

with

$$\mathbf{S}_{\mathbf{i}}^{\mathbf{aug}}\mathbf{S}_{\mathbf{o}}^{\mathbf{aug}} = \begin{bmatrix} \mathbf{S}_{\mathbf{i1}}^{\mathbf{aug}} \\ \mathbf{S}_{\mathbf{i2}}^{\mathbf{aug}} \end{bmatrix}, \quad \mathbf{S}_{\mathbf{o}}^{\mathbf{aug}} = \begin{bmatrix} \hat{\mathbf{S}} \\ \widetilde{\Delta\mathbf{S}} \end{bmatrix}.$$

Note that $\mathbf{S}_{\mathbf{i1}}^{\mathbf{aug}*}\mathbf{S}_{\mathbf{i1}}^{\mathbf{aug}} + \mathbf{S}_{\mathbf{i2}}^{\mathbf{aug}*}\mathbf{S}_{\mathbf{i2}}^{\mathbf{aug}} = \mathbf{I}_{\mathbf{L}}$ and $\mathbf{S}_{\mathbf{o}}^{\mathbf{aug}*}\mathbf{S}_{\mathbf{o}}^{\mathbf{aug}} = \hat{\mathbf{S}}^*\hat{\mathbf{S}} + \mathbf{\Phi}_{\Delta\mathbf{S}}$ which shows how $\mathbf{S_i}$ and $\mathbf{S_o}$ are adjusted to compensate for the model errors modeled by $\mathbf{\Phi}_{\Delta\mathbf{S}}$.

The next subsection describes how to estimate this robust filter by means of system identification.

4.2. Estimation of the robust filter

Using the models $\hat{\mathbf{S}}$ and $\widehat{\Delta\mathbf{S}} \in RH_\infty^{M\times M}$ which models $\widetilde{\Delta\mathbf{S}}$ such that $\widehat{\Delta\mathbf{S}}^*\widehat{\Delta\mathbf{S}} \approx \widetilde{\Delta\mathbf{S}}^*\widetilde{\Delta\mathbf{S}}$ we can define $\hat{\mathbf{S}}^{\mathbf{aug}}$ and its inner–outer factorization as

$$\hat{\mathbf{S}}^{\mathbf{aug}} := \begin{bmatrix} \hat{\mathbf{S}} \\ \widehat{\Delta\mathbf{S}} \end{bmatrix} = \begin{bmatrix} \hat{\mathbf{S}}_{\mathbf{i1}}^{\mathbf{aug}} \\ \hat{\mathbf{S}}_{\mathbf{i2}}^{\mathbf{aug}} \end{bmatrix} \hat{\mathbf{S}}_{\mathbf{o}}^{\mathbf{aug}}.$$

Then the Cautious Wiener filter $\mathbf{W_{CW}}$ can be estimated similar to Eq. (6) by

$$\hat{\mathbf{W}}_{\mathbf{CW}}(\hat{\mathbf{S}}^{\mathbf{aug}}, \hat{\mathbf{P}}_{\mathbf{o}}) = -\hat{\mathbf{S}}_{\mathbf{o}}^{\mathbf{aug}\dagger}[\hat{\mathbf{S}}_{\mathbf{i1}}^{\mathbf{aug}*}\hat{\mathbf{P}}_{\mathbf{o}}]_+\hat{\mathbf{P}}_{\mathbf{o}}^{-1}.$$

However, like in the case of the H_2 optimal filter, the factor $[\mathbf{S}_{\mathbf{i1}}^{\mathbf{aug}*}\mathbf{P}_{\mathbf{o}}]_+$ can also be estimated by system identification. By replacing $\mathbf{S_i}$ and $\mathbf{P_o}$ in the design of the nominal filter by $\hat{\mathbf{S}}_{\mathbf{i1}}^{\mathbf{aug}}$ and $\hat{\mathbf{P}}_{\mathbf{o}}$, respectively, it is inferred that $[\mathbf{S}_{\mathbf{i1}}^{\mathbf{aug}*}\mathbf{P}_{\mathbf{o}}]_+$ can be identified using input/output data

$$\{\hat{\mathbf{P}}_{\mathbf{o}}^{-1}\mathbf{d}(n), \hat{\mathbf{S}}_{\mathbf{i1}}^{\mathbf{aug}*}\mathbf{d}(n)\}_{n=1}^{N}.$$

The obtained estimate using $\hat{\mathbf{P}}_{\mathbf{o}}$ and $\hat{\mathbf{S}}_{\mathbf{i1}}^{\mathbf{aug}}$ and $N<\infty$ is denoted by $[\widehat{\mathbf{S}_{\mathbf{i1}}^{\mathbf{aug}*}\mathbf{P}_{\mathbf{o}}}]_+$. The estimate of the Cautious Wiener filter obtained by using $[\widehat{\mathbf{S}_{\mathbf{i1}}^{\mathbf{aug}*}\mathbf{P}_{\mathbf{o}}}]_+$ is given by

$$\hat{\mathbf{W}}_{\mathbf{CW,id}} = -\hat{\mathbf{S}}_{\mathbf{o}}^{\mathbf{aug}\dagger}[\widehat{\mathbf{S}_{\mathbf{i1}}^{\mathbf{aug}*}\mathbf{P}_{\mathbf{o}}}]_+\hat{\mathbf{P}}_{\mathbf{o}}^{-1}. \tag{17}$$

It can be shown, that this identification problem again is a control-relevant identification problem.

Finally, as in Section 3.3, an identification problem can be formulated to implicitly evaluate the multiplications in Eq. (17) to estimate a reduced order filter by system identification.

4.3. Estimation of the model error model

The secondary path model $\hat{\mathbf{S}}$ and the spectral factor $\widehat{\Delta\mathbf{S}}$ which models the uncertainty in the secondary path are estimated by means of a series of p experiments. In each experiment the (environmental) conditions may be different, e.g. in the experiments of Section 5 p is set to $p=2$ where the experiments are evaluated with and without an additional mass on a vibrating plate. In each experiment the secondary path is modeled, which yields a series of secondary path models $\{\hat{\mathbf{S}}^k\}_{k=1}^p$. Then, $\hat{\mathbf{S}}$ and $\widehat{\Delta\mathbf{S}}$ are determined such that

$$\hat{\mathbf{S}}(\mathrm{e}^{\mathrm{j}\omega}) = \frac{1}{p}\sum_{k=1}^{p}\hat{\mathbf{S}}^{\mathbf{k}}(\mathrm{e}^{\mathrm{j}\omega}), \quad \pi\leqslant\omega<\pi,$$

$$\widehat{\Delta\mathbf{S}}(\mathrm{e}^{\mathrm{j}\omega})^*\widehat{\Delta\mathbf{S}}(\mathrm{e}^{\mathrm{j}\omega}) = \frac{1}{p}\sum_{k=1}^{p}(\hat{\mathbf{S}}^{\mathbf{k}}(\mathrm{e}^{\mathrm{j}\omega}) - \hat{\mathbf{S}}(\mathrm{e}^{\mathrm{j}\omega}))^*(\hat{\mathbf{S}}^{\mathbf{k}}(\mathrm{e}^{\mathrm{j}\omega}) - \hat{\mathbf{S}}(\mathrm{e}^{\mathrm{j}\omega})), \quad -\pi\leqslant\omega<\pi.$$

To circumvent very high order models for $\hat{\mathbf{S}}$ and a high order spectral factorization problem for $\widehat{\Delta\mathbf{S}}$, $\hat{\mathbf{S}}$ and $\widehat{\Delta\mathbf{S}}$ are approximated by solving identification problems. $\hat{\mathbf{S}}$ of restricted order can be estimated using input/output data $\{\mathbf{u}(n), \mathbf{y}(n)\}_{n=1}^N$ with $\mathbf{u}(n)\in\mathbb{R}^K$ zero mean white noise and

$$\mathbf{y}(n) = \frac{1}{p}\sum_{k=1}^{p}\hat{\mathbf{S}}^{\mathbf{k}}\mathbf{u}(n).$$

The restricted order spectral factor $\widehat{\Delta\mathbf{S}}$ can be determined by estimating the spectrum of

$$\xi(n) = \frac{1}{\sqrt{p}}\sum_{k=1}^{p}(\hat{\mathbf{S}}^{\mathbf{k}} - \hat{\mathbf{S}})\zeta^{\mathbf{k}}(n)$$

with $\zeta^{\mathbf{k}}(n)$, $k=1,\ldots,p$ such that $E[\zeta^{\mathbf{k}}(n)] = \mathbf{0}$ and $E[\zeta^{\mathbf{k}}(n)\zeta^{\mathbf{kT}}(m)] = \mathbf{I_K}\delta(m-n)$ and $\zeta^{\mathbf{k}}$ independent of $\zeta^{\mathbf{l}}$ for $k\neq l$.

4.4. Stability robustness with respect to secondary path model errors

As is clear from Fig. 2, the closed-loop gain is given by

$$\mathbf{L}(\mathrm{e}^{-\mathrm{j}\omega}) = \mathbf{W}(\mathrm{e}^{-\mathrm{j}\omega})\Delta\mathbf{S}(\mathrm{e}^{-\mathrm{j}\omega}).$$

To guarantee stability in case $\Delta\mathbf{S}\neq\mathbf{0}$, a small gain argument can be inferred. According to the small gain Theorem (Zhou, Doyle, & Glover, 1996) stability is guaranteed if $\mathbf{W}\in RH_\infty^{K\times M}$, $\Delta\mathbf{S}\in RH_\infty^{M\times K}$ and the following inequality is satisfied:

$$\|\mathbf{W}(\mathrm{e}^{-\mathrm{j}\omega})\|_\infty < \frac{1}{\|\Delta\mathbf{S}(\mathrm{e}^{-\mathrm{j}\omega})\|_\infty}, \quad -\pi\leqslant\omega<\pi. \tag{18}$$

The assumption $\mathbf{W}\in RH_\infty^{K\times M}$ is satisfied because all factors in Eq. (16) are stable. Furthermore $\Delta\mathbf{S}\in RH_\infty^{M\times K}$ is satisfied in case $\mathbf{S}, \hat{\mathbf{S}}\in RH_\infty^{M\times K}$ which is usually the case in Active Control.

In the derivation of the CW filter, it is inferred that the gain of $\mathbf{W}$ is reduced in the frequency range where $\widehat{\Delta\mathbf{S}}$ (and thus on the average $\Delta\mathbf{S}$) is large to obtain robust performance. From (18) it is inferred that this is also needed for robust stability, i.e. for ω where $\|\Delta\mathbf{S}(\mathrm{e}^{\mathrm{j}\omega})\|_\infty$ is large $\|\mathbf{W}(\mathrm{e}^{\mathrm{j}\omega})\|_\infty$ should be small. However, the CW filter does not guarantee that Eq. (18) is satisfied, because (15) is not minimized subject to this constraint. To improve stability robustness an

Algorithm to estimate the robust controller for the plant in Figure 2

(1) Estimate models $\hat{\mathbf{S}}^{\mathbf{k}}$ using input/output data $\{\mathbf{u}(n), \mathbf{y}(n)\}_{n=1}^{N}$ with $\mathbf{s}(n) = 0$ under the conditions $k = 1, ..., p$;

(2) Estimate average model $\hat{\mathbf{S}} = \frac{1}{p}\sum_{k=1}^{p}\hat{\mathbf{S}}^{\mathbf{k}}$ and the spectral factor $\widehat{\Delta\mathbf{S}}$ such that $\widehat{\Delta\mathbf{S}}^{*}\widehat{\Delta\mathbf{S}} = \frac{1}{p}\sum_{k=1}^{p}(\hat{\mathbf{S}}^{\mathbf{k}} - \hat{\mathbf{S}})^{*}(\hat{\mathbf{S}}^{\mathbf{k}} - \hat{\mathbf{S}})$;

(3) Estimate model $\widehat{\mathbf{P}_o}$ using measurements $\{\mathbf{d}(n)\}_{n=1}^{N}$ with $\mathbf{u}(n) = 0$ under p conditions;

(4) Choose ρ and calculate inner-outer factorization of $\hat{\mathbf{S}}^{\mathbf{aug}} = \begin{bmatrix} \hat{\mathbf{S}} \\ \sqrt{\rho}\widehat{\Delta\mathbf{S}} \end{bmatrix}$;

(5) Estimate model $[\widehat{\mathbf{S}_{i1}^{aug*}\mathbf{P}_o}]_+$ using input/output data $\{\hat{\mathbf{P}}_o^{-1}\mathbf{d}(n), \hat{\mathbf{S}}_{i1}^{aug*}\mathbf{d}(n)\}_{n=1}^{N}$;

(6) Estimate (reduced order) filter $\widehat{\mathbf{S}_o^{aug-1}}[\widehat{\mathbf{S}_{i1}^{aug*}\mathbf{P}_o}]_+\widehat{\mathbf{P}_o^{-1}}$;

(7) Apply controller which consists of Wiener filter $\widehat{\mathbf{S}_o^{aug-1}}[\widehat{\mathbf{S}_{i1}^{aug*}\mathbf{P}_o}]_+\widehat{\mathbf{P}_o^{-1}}$ in closed loop with internal model $\hat{\mathbf{S}}$.

Fig. 3. Algorithm to estimate the robust controller for the plant in Fig. 2.

alternative cost function is introduced

$$J = \mathrm{tr}\, E[(\mathbf{d}(n) + \hat{\mathbf{S}}\mathbf{W}\mathbf{d}(n))(\mathbf{d}(n) + \hat{\mathbf{S}}\mathbf{W}\mathbf{d}(n))^{\mathrm{T}}] + \rho\, \mathrm{tr}\, E[(\widehat{\Delta\mathbf{S}}\mathbf{W}\mathbf{d}(n))(\widehat{\Delta\mathbf{S}}\mathbf{W}\mathbf{d}(n))^{\mathrm{T}}] \quad (19)$$

with $\rho > 0$ a scalar tuning variable. The cost function (15) equals (19) for $\rho = 1$. By increasing the value of ρ more weight is put on the second term and thus the gain of $\mathbf{W}$ will be more reduced. Note, that here the frequency dependency of $\Delta\mathbf{S}$ is explicitly taken into account, whereas in H_∞-theory the frequency dependency of model errors is implicitly taken into account by means of proper weighting functions. Furthermore, the introduction of the tuning parameter ρ is similar to the introduction of a user chosen ∞-norm bound (often indicated by γ) on the uncertainty; both parameters can be increased to improve stability robustness.

Fig. 3 summarizes the algorithm to estimate the robust controller described in this section.

5. Experimental validation on the vibrating plate

5.1. Description of the experimental setup

The nominal and the robust design method has been applied on a vibrating plate experimental setup, supplied by TNO Institute of Applied Physics, see Fig. 4. A loudspeaker is placed beneath the plate and generates a broadband disturbance sound, which propagates through the vibrating plate. The vibration of the plate should be counteracted by piezoelectric actuators mounted on the lower side of the plate. The residual vibration of the plate is measured by piezoelectric sensors mounted at the upper side of the plate, collocated with the actuators. In the experiments 4 sensors and 4 actuators are used as indicated in Fig. 4. The sampling frequency was $f_s = 2000$ Hz. The vibrating plate is controlled with the nominal and the robust controller under the two different operating conditions: without and with additional mass, of $\approx 6\%$ of the plate mass, mounted on the vibrating plate at the place between the 4 sensors.

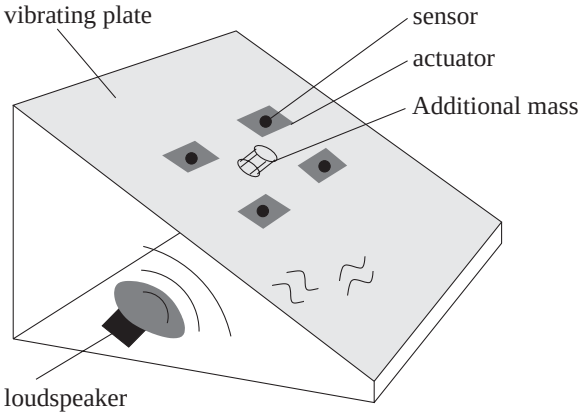

Fig. 4. Schematic picture of the vibrating plate setup of TNO TPD.

5.2. Identification of the average secondary path model and its variance

Under both conditions a state-space model $\hat{\mathbf{S}}^{\mathbf{i}}$ ($i = 1$: without mass, $i = 2$: with mass) of the secondary path was estimated using the PO-MOESP subspace model identification method (Verhaegen, 1994) using band limited white noise as the excitation signal. Here, a short description of the identification procedure is given, for a more detailed description of the procedure to identify models for active control applications, see Verdult and Fraanje (2002) or McKelvey, Fleming, & Moheimani (2002). Two input/output data sequences each of 14 000 samples (i.e. 7 s) were recorded, one for identification and the other for validation of the model. Both 4-inputs 4-outputs models $\hat{\mathbf{S}}^{\mathbf{1}}$ and $\hat{\mathbf{S}}^{\mathbf{2}}$ are of order 80 and accurately model the dynamics of the secondary path without and with additional mass mounted on the plate, respectively. A measure of the accuracy of the model is the Variance Accounted For (VAF), which is defined as

$$\mathrm{VAF}(\mathbf{y_{meas}}, \hat{\mathbf{S}}\mathbf{u}) := \left(1 - \frac{\mathrm{var}(\mathbf{y_{meas}} - \hat{\mathbf{S}}\mathbf{u})}{\mathrm{var}(\mathbf{y_{meas}})}\right)100\%,$$

where the calculations are performed per channel and with var(.) the variance operator, $\mathbf{y_{meas}}$ the measured output and $\hat{\mathbf{S}}\mathbf{u}$ the simulated output using the estimated model $\hat{\mathbf{S}}$ and the same input $\mathbf{u}$ applied during measurement of $\mathbf{y_{meas}}$. Table 1 gives the VAF values obtained

Table 1
VAF values (%) obtained by $\hat{\mathbf{S}}^{\mathbf{i}}$, $i = 1, 2$ and $\hat{\mathbf{S}}$ on validation data for the conditions with and without additional mass

	Output 1	Output 2	Output 3	Output 4
VAF($\mathbf{y}_{\text{no mass}}$, $\hat{\mathbf{S}}^{\mathbf{1}}\mathbf{u}$):	99.76	99.79	99.73	99.77
VAF($\mathbf{y}_{\text{with mass}}$, $\hat{\mathbf{S}}^{\mathbf{1}}\mathbf{u}$):	81.77	87.58	82.88	88.28
VAF($\mathbf{y}_{\text{no mass}}$, $\hat{\mathbf{S}}^{\mathbf{2}}\mathbf{u}$):	83.10	87.68	84.74	88.09
VAF($\mathbf{y}_{\text{with mass}}$, $\hat{\mathbf{S}}^{\mathbf{2}}\mathbf{u}$):	99.72	99.78	99.73	99.77
VAF($\mathbf{y}_{\text{no mass}}$, $\hat{\mathbf{S}}\mathbf{u}$):	95.39	96.66	95.76	96.71
VAF($\mathbf{y}_{\text{with mass}}$, $\hat{\mathbf{S}}\mathbf{u}$):	95.03	96.63	95.24	96.76

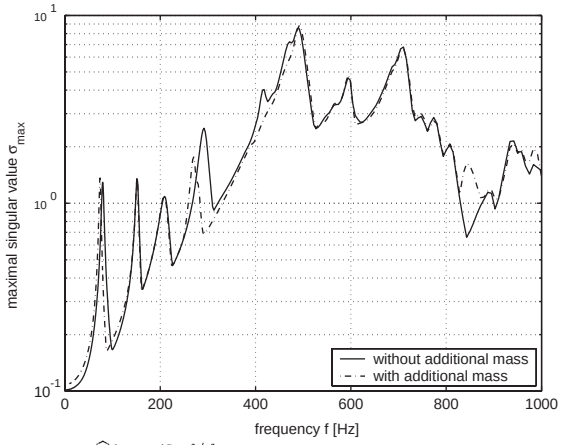

(a) $||\widehat{\mathbf{S}}^{\mathbf{1}}(e^{-j2\pi f/f_s})||_\infty$ (without mass added, solid) and $||\widehat{\mathbf{S}}^{\mathbf{2}}(e^{-j2\pi f/f_s})||_\infty$ (mass added, dashed).

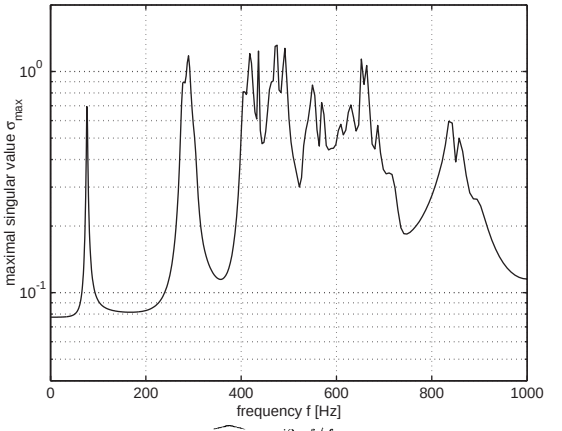

(b) $||\widehat{\Delta\mathbf{S}}(e^{-j2\pi f/f_s})||_\infty$.

Fig. 5. Maximal singular value of estimated model with and without mass (a) and their difference (b).

using $\hat{\mathbf{S}}^{\mathbf{i}}$, $i = 1, 2$ and $\hat{\mathbf{S}} \approx (\hat{\mathbf{S}}^{\mathbf{1}} + \hat{\mathbf{S}}^{\mathbf{2}})/2$ on validation data measured under both conditions with, $\mathbf{y}_{\text{with mass}}$, and without additional mass, $\mathbf{y}_{\text{no mass}}$. It can be concluded, that the model obtained under no additional mass condition is not accurate anymore under the additional mass condition and vice verse. The average model $\hat{\mathbf{S}}$ models both conditions much better, but still has significant model errors for which the controller should be robust.

Fig. 5(a) shows the largest singular value of $\hat{\mathbf{S}}^{\mathbf{i}}(e^{-j2\pi f/f_s})$, $i = 1, 2$, which shows that the first and the fourth resonance frequencies significantly change in case an additional mass is mounted. The average secondary path model $\hat{\mathbf{S}}$ and the model error model $\widehat{\Delta\mathbf{S}}$ are estimated as described in Section 4.3. The average model $\hat{\mathbf{S}}$ has order 80, and $\widehat{\Delta\mathbf{S}}$ has order 50. Fig. 5(b) shows the largest singular value $||\widehat{\Delta\mathbf{S}}(e^{-j2\pi f/f_s})||_\infty$. It is clearly seen, that the model error is depending on the frequency.

5.3. Estimation of the average spectral factor of the disturbance

The spectral factor $\mathbf{P_o}$ of the disturbance signal changes when an additional mass is mounted on the vibrating plate. Therefore, like in modeling the secondary path, an average model of the spectral factor $\mathbf{P_o}$ has been estimated by averaging the measured disturbances under both conditions. The estimated spectral factor model $\hat{\mathbf{P}}_\mathbf{o}$ has order 40. The filter $\hat{\mathbf{P}}_\mathbf{o}^{-1}$ is an approximation of the whitening filter for the disturbance signal. Fig. 6 shows the spectra of the disturbance signal of output 1 (dashed) and the spectrum obtained by using the whitening filter $\hat{\mathbf{P}}_\mathbf{o}^{-1}$ (solid) for the average disturbance, the measured disturbance without additional mass and the measured disturbance with additional mass respectively.

From these figures it can be concluded that $\hat{\mathbf{P}}_\mathbf{o}^{-1}$ indeed approximately whitens the disturbance signal under both conditions. However at 300 and 600 Hz there are still resonances in the whitened disturbance signal, which are due to the fact that the spectrum of the disturbance signal differs under both conditions. At high frequencies, above ≈ 700 Hz, the spectrum of the disturbance signal falls down.

5.4. Nominal and robust controller estimation and validation

5.4.1. Nominal controller estimation and validation

Using $\hat{\mathbf{P}}_\mathbf{o}$ and $\hat{\mathbf{S}}$, the Causal Wiener filter Eq. (5) can be calculated explicitly. After model reduction, a 120th order filter has been obtained. The performance measure is the average performance over the whole frequency band in dB, which is defined as

$$-10^{10}\log\frac{1}{M}\sum_{k=1}^{M}\frac{1}{2\pi}\int_{-\pi}^{\pi}\frac{\mathbf{\Phi}_{\mathbf{e_k}}(\omega)}{\mathbf{\Phi}_{\mathbf{d_k}}(\omega)}\mathrm{d}\omega \tag{20}$$

with $\mathbf{\Phi}_{\mathbf{d_k}}$ and $\mathbf{\Phi}_{\mathbf{e_k}}$ the power spectra of the kth disturbance signal and the kth residual signal, respectively. The average performance over the whole frequency band for each output separately and based on simulation (hence there is no measurement noise and the secondary path is perfectly modeled) using the average disturbance signal is given in Table 2.

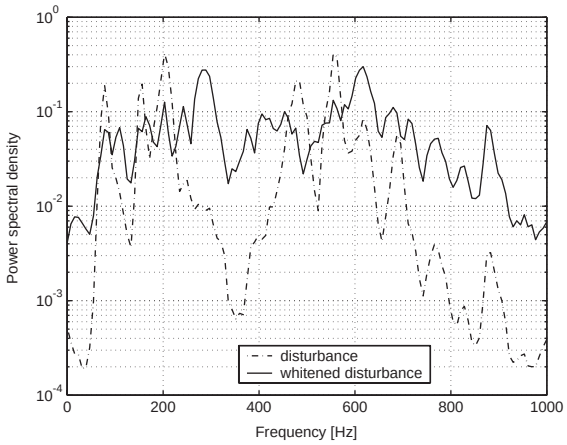

(a) Average disturbance and whitened.

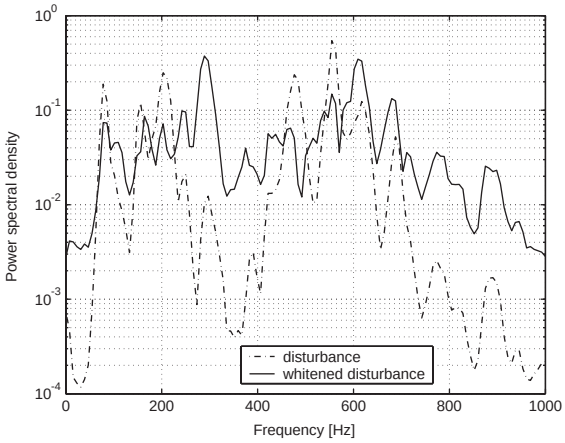

(b) Disturbance without additional mass and whitened.

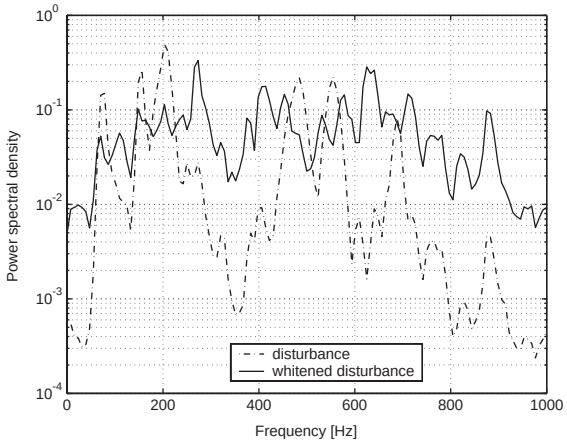

(c) Disturbance with additional mass and whitened.

Fig. 6. Spectrum of disturbance at output 1 under various conditions (dashed) and pre-whitened (solid).

Table 2
Average reduction in dBs of the H_2 optimal controller, the identified H_2 optimal controller and the identified reduced order filter obtained by simulation

	Output 1	Output 2	Output 3	Output 4
H_2 optimal (order = 120):	6.9	8.1	6.5	7.6
Identified H_2 optimal (order = 160):	7.1	8.7	7.0	8.1
Identified (reduced order, order = 80):	7.1	8.6	6.8	7.7

The H_2 optimal controller can also be estimated using the identification approach described in Section 3.3. The factor $[\mathbf{S}_\mathbf{i}^*\mathbf{P}_\mathbf{o}]_+$ was estimated by causal-/anti-causal subspace identification, using 14 000 samples and 100 block rows, the estimate of the order is 56. Because 16 anti-causal poles of $\mathbf{S}_\mathbf{i}^*\mathbf{P}_\mathbf{o}$ which are due to $\mathbf{S}_\mathbf{i}^*$ are rejected, the order of $\widehat{[\mathbf{S}_\mathbf{i}^*\mathbf{P}_\mathbf{o}]_+}$ is 40. The controller obtained by explicitly evaluating the multiplications in Eq. (5) is 160. The performance of this controller is given in the second row in Table 2. A reduced order filter of order 80 could be estimated by formulating the controller order reduction problem as an identification problem (see Section 3.3). Its simulated performance is given by the third row in Table 2.

From Table 2. it can be concluded that the performance of the identified H_2 optimal controller (based on simulation) is better than the performance of the explicitly calculated H_2 optimal controller. This can be explained by the fact that in the identification approach a control-relevant identification problem is solved which compensates for model errors in $\hat{\mathbf{P}}_\mathbf{o}$. Furthermore, the order of the identified controller could be reduced by about a factor 2 (from 160 to 80), without (significant) performance loss.

By applying the 80th (reduced) order identified controller into the real-time setup to control the vibrating plate, the closed-loop became unstable under both conditions: without and with the additional mass mounted on the plate, which is due to the relatively large model error in the average model $\hat{\mathbf{S}}$ for both conditions. This motivates the use of a robust controller.

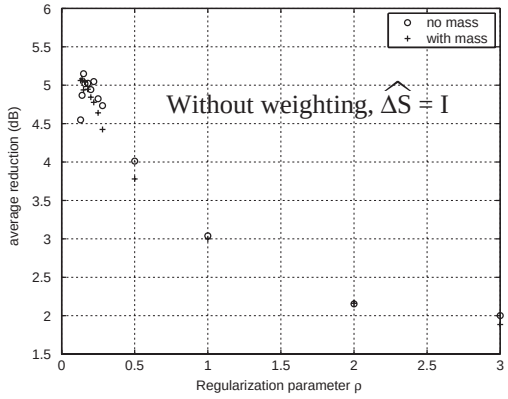

(a) Average reduction verus ρ without weighting ($\Delta S = I$).

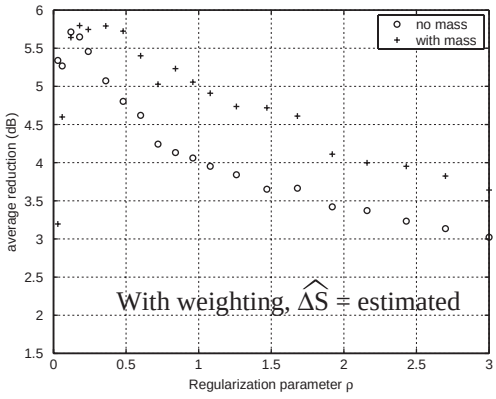

(a) Average reduction verus ρ with weighting (ΔS estimated).

Fig. 7. Average performance (20) over all outputs (dB) versus regularization parameter ρ *without* (a) and *with* (b) weighting with the estimated $\widehat{\mathbf{\Delta S}}$ for the case without additional mass (o's) and with additional mass (+'s).

5.4.2. Robust controller estimation and validation

The robust controller was determined in two different ways. One way is to minimize the cost function Eq. (19) with setting $\widehat{\mathbf{\Delta S}} = \mathbf{I}$, which is equivalent with standard control weighting, see e.g. Elliott (2001). The other way is minimizing (19), with $\widehat{\mathbf{\Delta S}}$ determined in Section 5.2. In both methods the value of ρ was varied to increase (and decrease) robustness.

Like in the design of the nominal controller, the order of the robust controllers was reduced to 80 by means of solving an identification problem. Fig. 7(a) shows the measured average reduction in dBs over all 4 outputs versus ρ obtained by the controller with $\widehat{\mathbf{\Delta S}} = \mathbf{I}$, i.e. frequency independent regularization, for the case without (o's) and with (+'s) additional mass. For $\rho \geqslant 0.13$ it is observed that the closed loop was stabilized by the controller. Fig. 7(b) shows the measured average reduction in dBs over all 4 outputs versus ρ obtained by the controller with $\widehat{\mathbf{\Delta S}}$ estimated in Section 5.2, i.e. frequency-dependent regularization, also for the case without (o's) and with (+'s) additional mass. In this figure, ρ is scaled with a factor 33 for visualization reasons. The maximum performance is obtained for $33\rho = 5, \ldots, 10$ for the cases with and without additional mass. Note, that for maximum performance, the weighting $33\rho > 1$ to increase stability robustness.

Comparing both figures, it is concluded that using $\widehat{\mathbf{\Delta S}}$ estimated in Section 5.2 yields better performance. This is also what is expected, because the reduction of the control effort is emphasized only at the critical frequencies (i.e. where the uncertainty is large).

6. Conclusions

The H_2 optimal controller for feedback systems was estimated from signals that can easily be recorded. The estimation was carried out using the IMC principle and the solution of a control-relevant identification problem. Using the probabilistic robust feed forward controller/filter design method, a robust controller has been identified. The model error (of the secondary path model) is assumed to be a zero-mean stochastic variable, of which the covariance function is known. By minimizing the mean-squared error averaged over the distribution of the model uncertainty, a robust filter has been designed which yields increased robust performance. Because the gain of this filter has been reduced in the frequency region where the model uncertainty is large, the loop gain has been reduced which yields increased stability robustness.

The robust controller design method was illustrated on a MIMO vibrating plate experimental setup without and with additional mass. The nominal controller did not stabilize the closed loop. By introducing sufficient control weighting the closed-loop was stabilized. It has also been shown that weighting the control signal with the probabilistic model error model could lead to a less conservative controller and hence better performance could be obtained.

Future research will be directed to the problem to iteratively update the controller and secondary path model with its model error with the final goal to obtain optimal performance for the specific conditions of the plant.

Acknowledgements

The authors want to thank Dr. Ir. X.J.A. Bombois from Delft Center of Systems and Control, Delft University of Technology, The Netherlands, for the fruitful discussions and comments.

Appendix A. Proofs

A.1. Proof of Lemma 3

The proof follows directly by noting that

$$
\begin{aligned}
&J(\mathbf{C}(\mathbf{W}(\mathbf{X}),\mathbf{S}))\\
&\quad=\frac{1}{2\pi}\operatorname{tr}\int_{-\pi}^{\pi}(\mathbf{P_o}+\mathbf{SW}(\mathbf{X})\mathbf{P_o})(\mathbf{P_o}+\mathbf{SW}(\mathbf{X})\mathbf{P_o})^*\,\mathrm{d}\omega\\
&\quad=\frac{1}{2\pi}\operatorname{tr}\int_{-\pi}^{\pi}(\mathbf{P_o}-\mathbf{S_i}\mathbf{X}\mathbf{P_o})^*[\mathbf{S_i}\ \mathbf{S_i}^{\perp}][\mathbf{S_i}\ \mathbf{S_i}^{\perp}]^*(\mathbf{P_o}-\mathbf{S_i}\mathbf{X}\mathbf{P_o})\,\mathrm{d}\omega\\
&\quad=\frac{1}{2\pi}\operatorname{tr}\int_{-\pi}^{\pi}\mathbf{S_i}^{\perp *}\mathbf{P_o}\mathbf{P_o}^*\mathbf{S_i}^{\perp}\,\mathrm{d}\omega\\
&\qquad+\frac{1}{2\pi}\operatorname{tr}\int_{-\pi}^{\pi}(\mathbf{S_i}^*\mathbf{P_o}-\mathbf{X}\mathbf{P_o})^*(\mathbf{S_i}^*\mathbf{P_o}-\mathbf{X}\mathbf{P_o})\,\mathrm{d}\omega\\
&\quad=\frac{1}{2\pi}\operatorname{tr}\int_{-\pi}^{\pi}\mathbf{S_i}^{\perp *}\mathbf{P_o}\mathbf{P_o}^*\mathbf{S_i}^{\perp}\,\mathrm{d}\omega+J_{id}(\mathbf{X})
\end{aligned}
$$

with $\mathbf{S_i}^{\perp}$ such that $[\mathbf{S_i}\ \mathbf{S_i}^{\perp}]$ is unitary. Hence, minimizing $J_{id}(\mathbf{X})$ over $\mathbf{X}\in RH_{\infty}^{L\times M}$ is equivalent to minimizing $J(\mathbf{C}(\mathbf{W}(\mathbf{X}),\mathbf{S}))$ over $\mathbf{X}\in RH_{\infty}^{L\times M}$.

A.2. Proof of Theorem 4

By transforming Eq. (15) to the frequency domain and using the fact that $\Delta\mathbf{S}$ is independent of $\mathbf{s}(n)$, $\mathbf{P}$ and $\hat{\mathbf{S}}$ the expression for J_{rob} can be written as

$$
\begin{aligned}
J_{\mathrm{rob}}&=\frac{1}{2\pi}\operatorname{tr}\int_{-\pi}^{\pi}(.)^*(\mathbf{P}+\hat{\mathbf{S}}\mathbf{W_{CW}}\mathbf{P})+\ \mathbf{P}^*\mathbf{W_{CW}}^*\mathbf{\Phi}_{\Delta\mathbf{S}}\mathbf{W_{CW}}\mathbf{P}\,\mathrm{d}\omega\\
&=\frac{1}{2\pi}\operatorname{tr}\int_{-\pi}^{\pi}(.)^*(\mathbf{P}+\hat{\mathbf{S}}\mathbf{W_{CW}}\mathbf{P})+\ \mathbf{P}^*\mathbf{W_{CW}}^*\widetilde{\Delta\mathbf{S}}^*\widetilde{\Delta\mathbf{S}}\mathbf{W_{CW}}\mathbf{P}\,\mathrm{d}\omega\\
&=\frac{1}{2\pi}\operatorname{tr}\int_{-\pi}^{\pi}(\mathbf{P_o}+\hat{\mathbf{S}}\mathbf{W_{CW}}\mathbf{P_o})(.)^*+\ \widetilde{\Delta\mathbf{S}}\mathbf{W_{CW}}\mathbf{P_o}\mathbf{P_o}^*\mathbf{W_{CW}}^*\widetilde{\Delta\mathbf{S}}^*\,\mathrm{d}\omega\\
&=\frac{1}{2\pi}\operatorname{tr}\int_{-\pi}^{\pi}(\mathbf{P_o^{aug}}+\mathbf{S^{aug}}\mathbf{W_{CW}}\mathbf{P_o})(.)^*\,\mathrm{d}\omega \qquad \text{(A.1)}
\end{aligned}
$$

Using the solution of the nominal H_2 feed forward controller design problem of Theorem 1, it directly follows that $\mathbf{W_{CW}}\in RH_{\infty}^{K\times M}$ minimizes J_{rob} if $\mathbf{W_{CW}}$ is given by Eq. (16).

References

Anderson, B. D. O., & Moore, J. B. (1989). *Optimal control—linear quadratic methods*. Englewood Cliffs, NJ: Prentice Hall International Editions.

Bernstein, D. S., & Haddad, W. M. (1989). LQG control with an H_∞ performance bound: A Riccati equation approach. *Transactions on Automatic Control*, *AC-34*(3), 293–305.

Elliott, S. J. (2001). *Signal processing for active control*. London, UK: Academic Press.

Fraanje, R., Verhaegen, M., & Doelman, N. J. (2001). *MIMO H_2 optimal controller design by subspace identification for active control applications*. Internal report UT/TN/SCE-2001-11, University of Twente, The Netherlands.

Gevers, M., & Li, G. (1993). *Parametrizations in control, estimation and filtering problems: Accuracy aspects*. Communication and control engineering series. New York: Springer.

Goodwin, G. C., Gevers, M., & Ninnes, B. (1992). Quantifying the error in estimated transfer functions with application to model order selection. *IEEE Transactions on Automatic Control*, *AC-37*(7), 913–928.

Ljung, L. (1999). *System identification—theory for the user*. Upper Saddle River, NJ, USA: Prentice Hall.

Ljung, L. (2002). *System identification toolbox—for use with Matlab, user's guide version* (5th ed.). Natick, MA, USA: The Mathworks.

Mari, J., Stoica, P., & McKelvey, T. (2000). Vector ARMA estimation: A reliable subspace approach. *IEEE Transactions on Signal Processing*, *SP-48*(7), 2092–2104.

McKelvey, T., Fleming, A., & Moheimani, S. (2002). Subspace-based system identification for an acoustic enclosure. *Transactions of the ASME, Journal of Vibration and Acoustics*, *124*(3), 414–419.

Örn, K. (1996). *Design of multivariable cautious discrete-time Wiener filters*. Ph.D. thesis, Uppsala University.

Paganini, F. (1999). Convex methods for robust H_2 analysis of continuous-time systems. *IEEE Transactions on Automatic Control*, *AC-44*(2), 239–252.

Petersen, I. R., Ugrinovskii, V., & Savkin, A. V. (2000). *Robust control design using H_∞ methods*. London, UK: Springer.

SLICOT (2002). *Niconet international society: The SLICOT package*. Secretariat: Mrs. Ida Tassens, Department of Electrical Engineering, Katholieke Universiteit Leuven, Kasteelpark Arenberg 10, 3001 Leuven, Belgium. http://www.win.tue.nl/niconet/.

Sternad, M., & Ahlén, A. (1993). Robust filtering and feedforward control based on probabilistic descriptions of model errors. *Automatica*, *29*(3), 661–679.

Verdult, V., & Fraanje, R. (2002). Slicot determines models for active noise control. '*NICONET Newsletter*' number 8, Working Group on Software WGS, pp. 13–18. http://www.win.tue.nl/niconet.

Verhaegen, M. (1994). Identification of the deterministic part of MIMO state space models given in innovations form from input-output data. *Automatica*, *30*(1), 61–74.

Verhaegen, M. (1996). A subspace model identification solution to the identification of mixed causal anti-causal lti systems. *SIAM Journal on Matrix Analysis*, *17*(2), 332–347.

Vidyasagar, M. (1985). *Control systems synthesis: A factorization approach*. Cambridge, MA, USA: The MIT Press.

Zhou, K., Doyle, J. C., & Glover, K. (1996). *Robust and optimal control*. Englewood Cliffs, NJ: Prentice Hall.